Factors altering the affinity of protein–ligand binding in an external electrostatic field

CrossMark

Shyh-Ming Kuo, Pei-Kun Yang *

Department of Biomedical Engineering, College of Medicine, I-SHOU University, Kaohsiung 82445, Taiwan, ROC

A R T I C L E   I N F O

A B S T R A C T

The effects of an external electric field on the binding affinity for protein–ligand complexes was determined by applying electric field E^{ext} to a water cluster containing two electric dipoles separated by a certain distance. The mean forces on these two dipoles were computed from the trajectories of molecular dynamics simulations. The results showed that the mean attractive force and the binding affinity between these two dipoles decreased with increasing E^{ext}. Two factors governing the effects of E^{ext} on the binding affinity of protein–ligand interactions were proposed. (1) When E^{ext} is applied to a water cluster containing protein–ligand complexes, the water molecules neighboring ligand will be repelled from the ligand; the mean van der Waals repulsive force exerted on the ligand by these water molecules would decrease, leading to a decrease in the binding affinity between the protein and the ligand. (2) The mean electrostatic force exerted on the ligand by the water molecules polarized by E^{ext} is thought to result from the dielectric polarization ($P_{protein}$) in the region occupied by the protein, where $P_{protein}$ is proportional to $-E^{ext}$.

1. Introduction

Various devices used for convenience in daily life are powered by electricity. These electrical devices generate electromagnetic radiation. The power lines that transmit electrical power from power plants to cities also generate large amounts of low-frequency electromagnetic radiation. Electromagnetic radiation from power lines, cell phones, microwave ovens, hair dryers, and other home appliances may be harmful to humans, because electric force dominates the interactions between atoms in biomolecules such as proteins, DNA, and RNA. Electromagnetic radiation can be reduced using various methods; however, these methods are not generally cost-effective. Understanding the effect of electromagnetic radiation on humans is helpful in determining the level of effort required to reduce electromagnetic radiation.

Consider the cell under an external electric field (E^{ext}); E^{ext} will alter the electric force on the biomolecule atoms and the polarization of water molecules present in the cell. It may also disturb the binding affinity of protein–protein/ligand interactions, stability of protein conformations, activity of proteins, and expression of biomolecules in organisms. Although these effects may not immediately induce diseases in humans, they may increase the possibility of diseases. At the same time, E^{ext} also has many useful applications; for example, it may be used to destroy bacteria and thus aid in food preservation. The dangers of E^{ext} have previously been studied [1] by protein experiments [2–6],

cell experiments [7–10], animal experiments [11], and public health studies [12].

Most biomolecules, including proteins, DNA, and RNA, exist in an aqueous environment. Water molecules have a large permanent electric dipole moment and can be rotated and translated freely in solution. Water molecules polarized by charged atoms can shield the atoms from the electric interactions that occur between the charged atoms. For two charged atoms separated by a large distance, the electric force between them in water is 1/80 of the equivalent electric force in a vacuum. Another effect of water is to reduce the contact area between the hydrophobic part of solutes and water molecules. Water molecules readily form hydrogen bonds with neighboring water molecules. The hydrophobic part of the solute breaks the hydrogen bonds among the water molecules. Therefore, the hydrophobic interactions play an important role in the stability of protein conformations and binding affinity of protein–protein/ligand interactions [13]. Many strategies had been developed to treat these solvent effects, and can be classified as explicit [14], hybrid [15–18], or implicit [19–27] solvent models. The most popular method used in recent years to calculate protein–ligand binding affinities was based on an implicit solvent model such as Molecular Mechanics/Poisson–Boltzmann Surface Area (MM/PBSA) and Molecular Mechanics/Generalized Born Surface Area (MM/GBSA) [28–32].

The effect of E^{ext} on the stability of protein conformations has previously been studied using molecular dynamics (MD) simulations [33–36]. The effects of E^{ext} on the stability of β sheet structures, dependence of E^{ext} on the polarization of water molecules, mean force on the charged atom in a water cluster, and interaction forces between two

* Corresponding author.
E-mail address: peikun@isu.edu.tw (P.-K. Yang).

charged or neutral atoms in a water cluster have been explored using MD simulations [37,38]. Maxwell's equations have been modified for treating the electromagnetic interactions between molecular solutes [39]. Hydrogen bonds play an important role in the stability of protein conformations and binding affinity of protein–protein/ligand interactions. To understand the bases of these hydrogen interactions, E^{ext} was applied to a water cluster containing two electric dipoles exposed to or buried in water. This was done to mimic the interactions between the hydrogen-bond donor and acceptor; the factors that govern the effects of E^{ext} on protein–ligand interactions were proposed.

2. Method

2.1. Molecular dynamics simulations

The source code of the CHARMM package [40] was modified and applied in the following scenarios to verify that it could be applied to an E^{ext}. (1) E^{ext} was applied to a simulation system containing one or two charged atoms in a vacuum. The results showed that the accelerations, velocities, and positions of atoms from MD simulations using the modified CHARMM were consistent with those obtained from analytical solutions (data not shown). (2) E^{ext} was applied to a pure water cluster, and the relation between the time-averaged dipole moment of water molecules and the time-averaged electric field at the water molecules was consistent with the results obtained in previous works [41,42].

In this project, $E^{ext} = 0$, 40, 60, or 100 MV cm^{-1} was applied to a water cluster with radius $R_{cluster} = 2$ nm, containing two exposed (D^I, D^{II}) (Scheme 1a) or buried (D^{III}, D^{IV}) (Scheme 1b) electric dipoles. The center of the two dipoles was at the center of a water cluster. The distance, d, by which the two dipoles were separated in the x direction ranged from 0.3 to 0.6 nm at intervals of 0.02 nm. The electric dipoles, with an amplitude of dipole moment of $8 * 10^{-30}$ C m, were mimicked by two charged atoms with charge $-1.6 * 10^{-19}$ and $+1.6 * 10^{-19}$ C separated by a distance of 0.05 nm. The van der Waal (vdW) parameters of atoms in D^I and D^{II} were assigned the same values as those of the oxygen atom of TIP3P water; this is because the vdW radii of N, Cα, C, and O atoms in the amino acids and that of the oxygen atom of TIP3P water are similar, with $\varepsilon = -0.6364$ kJ mol^{-1}, and $R_{min}/2 = 0.17682$ nm and $R_{min}/2 = 0.4$ nm for D^{III} and D^{IV}. The simulations were carried out in an NVE (i.e., moles (N), volume (V), and energy (E)) ensemble using the CHARMM package [40] and spherical boundary conditions without cutoff. The ion–water and water–water interaction energies were calculated by using the sum of electric and vdW pairwise energies. The O–H bond length (0.09572 nm) and H–O–H bond angle (104.52°) of the TIP3P water molecule were constrained during the simulations performed using the SHAKE algorithm [43]. The two exposed or buried electric dipoles were fixed during the MD simulations; the other atoms propagated according to Newton's equations using the leapfrog Verlet algorithm and a time step of 2 fs at a mean temperature of 300 K. Each of the systems was first minimized for 1000 steps, equilibrated for 200 ps, and then subjected to 4 ns of production dynamics. The configurations were stored every 20 fs.

2.2. Calculation of the mean forces

E^{ext} was applied to the water cluster containing D^I and D^{II}. Its contributions to the mean force on D^I (F^I) were as follows: the contribution from E^{ext} ($F^{I,E}$) and D^{II} ($F^{I,II}$); the contribution from the solvent molecules ($F^{I,solv}$) was computed using the MD-simulation trajectories. $F^{I,E}$ was zero because the net charge of D^I was zero. Therefore, F^I can be computed as follows:

$$F^I = F^{I,II} + F^{I,solvent}. \tag{1}$$
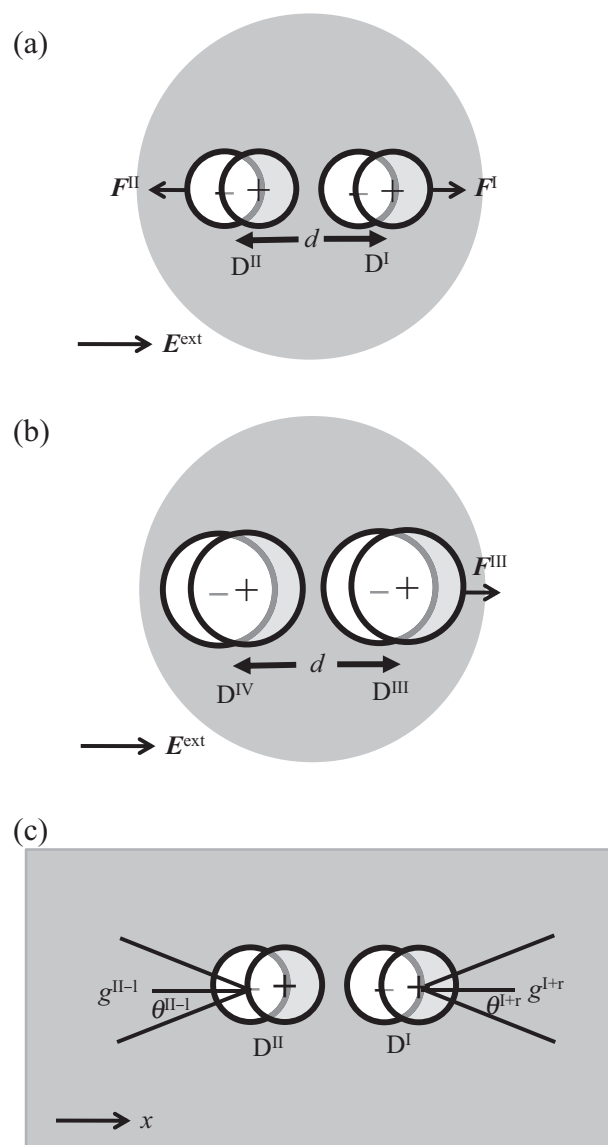
Scheme 1. (a) E^{ext} is applied to a water cluster (gray background) containing D^I and D^{II}. D^I contains two atoms with charges $-1.6 * 10^{-19}$ and $+1.6 * 10^{-19}$ C positioned at $(x, y, z) = (d/2 - 0.025$ nm, 0, 0) and $(d/2 + 0.025$ nm, 0, 0), respectively. D^{II} contains two atoms with charges $-1.6 * 10^{-19}$ and $+1.6 * 10^{-19}$ C positioned at $(x, y, z) = (-d/2 - 0.025$ nm, 0, 0) and $(-d/2 + 0.025$ nm, 0, 0), respectively. F^I and F^{II} are the mean forces on D^I and D^{II}, respectively. (b) E^{ext} is applied to the water cluster containing D^{III} and D^{IV}, with van der Waals radii of the atoms assigned double that of the oxygen atom of TIP3P. F^{III} is the mean force on D^{III}. (c) The relative solvent molecular densities are calculated on the right side of D^{I+} (g^{I+r}) and left side of D^{II-} (g^{II-l}). g^{I+r} and g^{II-l} are calculated from the water molecules in the region $\theta^{I+r} < 36°$ and $\theta^{II-l} < 36°$, respectively.

$F^{I,II}$ can be computed as the sum of the electric component ($F^{I,II}_{ele}$) and vdW component ($F^{I,II}_{vdW}$) as follows:

$$F^{I,II}_{ele} = \frac{1}{N_C} \sum_{l=1}^{N_C} \sum_{i=1}^{N_I} \sum_{j=1}^{N_{II}} \frac{q_i^I q_j^{II} R_{ij}^l}{4\pi\varepsilon_0 \left(R_{ij}^l\right)^3} \tag{2}$$

$$F^{I,II}_{vdW} = \frac{1}{N_C} \sum_{l=1}^{N_C} \sum_{i=1}^{N_I} \sum_{j=1}^{N_{II}} \frac{12\varepsilon_{ij}}{R_{ij}^l} \left[\left(\frac{R_{min,ij}}{R_{ij}^l}\right)^{12} - \left(\frac{R_{min,ij}}{R_{ij}^l}\right)^6\right] \frac{R_{ij}^l}{R_{ij}^l} \tag{3}$$

where q_i^I is the charge state of atom i in D^I, q_j^{II} is the charge state of atom j in D^{II}, and N_I and N_{II} represent the number of atoms in D^I and D^{II}, respectively. N_C is the number of configurations collected in the MD